

Resonance Raman Characterization of Iron(III) Porphyrin *N*-Oxide: Evidence for an Fe–O–N Bridged Structure[†]

Yasuhisa Mizutani,^{1,a,b} Yoshihito Watanabe,^{1,c} and Teizo Kitagawa^{1,a,b}

Contribution from the Institute for Molecular Science, Okazaki National Research Institutes, and Department of Functional Molecular Science, School of Mathematical and Physical Science, the Graduate University for Advanced Studies, Okazaki 444, Japan, and Division of Molecular Engineering, Graduate School of Engineering, Kyoto University, Sakyo, Kyoto 606, Japan

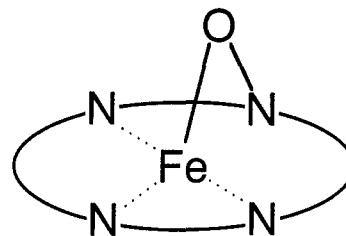
Received May 18, 1993[⊙]

Abstract: Resonance Raman (RR) spectra are reported for iron(III) tetramesityl porphyrin (TMP) *N*-oxide and its ¹⁸O and ¹⁵N derivatives. The RR bands assignable to the Fe–O stretching, O–N stretching, and Fe–O–N bending vibrations were observed at 506, 1122, and 743 and 708 cm⁻¹, respectively. This confirms that the complex has the Fe–O–N bridged structure. The RR bands of the macrocycle such as the C_βC_β and C_αN stretching modes were split into doublets due to lowering of symmetry. The RR band arising from the C_m–phenyl stretching band exhibited a downshift by 4 cm⁻¹ upon formation of the *N*-oxide, suggesting considerable distortion of the macrocycle.

Introduction

The mechanism of dioxygen activation by cytochrome P-450 (P-450) has been a subject of considerable interest in recent years.² While the presence of the oxy–ferrous complex in the mechanism has been demonstrated,³ successive intermediates have still remained to be characterized. An oxo–ferryl porphyrin π cation radical having monooxygenase activity⁴ is the most likely candidate for the ultimate oxygenating intermediate, and its physicochemical properties have been extensively investigated with XAFS,⁵ Mossbauer,⁶ NMR,⁷ and resonance Raman⁸ (RR) techniques. An alternative intermediate of the active species is an N-bridged iron–porphyrin (Fe–P) *N*-oxide, as illustrated in Scheme 1, which was suggested from the studies on N-bridged Fe–P carbene adducts⁹ and *N*-oxides of Ni(II) and Cu(II) porphyrins.^{10,11} MO calculations predicted that Fe^{III}-P *N*-oxide is more stable than the isomeric Fe^{IV}=O porphyrin π cation

Scheme 1



1

radical.¹² Groves and Watanabe¹³ first synthesized the Fe^{III}-P *N*-oxide and pointed out that this complex has no monooxygenase activity^{13b} and is likely to be an intermediate in suicide reactions of P-450.¹⁴ Recently, Tsurumaki et al.¹⁵ demonstrated that the Fe^{III}-P *N*-oxide has a high-spin ferric-iron with large rhombicity from the observation of β -pyrrole deuterium resonances in the downfield region (41.2, 71.7, 106, and 126 ppm) of NMR spectra and well-defined peaks at $g = 9.0, 5.0, 3.8,$ and 3.5 in EPR spectra, leading to a large E/D value ($=0.20$). Despite extensive applications of RR spectroscopy to heme proteins,¹⁶ there has been no RR data reported for an Fe–P *N*-oxide. In this study we have observed the isotopic frequency shifts of Raman bands for the N-bridged Fe–P *N*-oxide for the first time and assigned the Fe–O stretching ($\nu_{\text{Fe-O}}$), O–N stretching ($\nu_{\text{O-N}}$), and Fe–O–N bending ($\delta_{\text{Fe-O-N}}$) vibrations.

Experimental Section

(5,10,15,20-tetramesitylporphyrinato)-Fe^{III} hydroxide [(TMP)Fe^{III}-OH] and its ¹⁵N-substituted [(¹⁵N₄-TMP)Fe^{III}-OH] and ⁵⁴Fe-substituted

- * Author to whom correspondence should be addressed.
[†] This study was supported by a Grant-in-Aid from the Ministry of Education, Science, and Culture, Japan, to Priority Areas (Bioinorganic Chemistry 03241105) to T.K.
[⊙] Abstract published in *Advance ACS Abstracts*, March 15, 1994.
 (1) (a) Institute for Molecular Science. (b) The Graduate University for Advanced Studies. (c) Kyoto University.
 (2) McMurry, T. J.; Groves, J. T. In *Cytochrome P-450: Structure, Mechanism, and Biochemistry*; Ortiz de Montellano, P. R., Ed.; Plenum Press; New York, 1986; Chapter 1.
 (3) (a) Ishimura, Y.; Ullrich, V.; Peterson, J. A. *Biochem. Biophys. Res. Commun.* **1971**, *42*, 140–146. (b) Peterson, J. A.; Ishimura, Y.; Griffin, B. W. *Arch. Biochem. Biophys.* **1972**, *149*, 197–208. (c) Bangcharoenpauprong, O.; Rizos, A. K.; Champion, P. M. *J. Biol. Chem.* **1986**, *261*, 8089–8092. (d) Egawa, T.; Ogura, T.; Makino, R.; Ishimura, Y.; Kitagawa, T. *J. Biol. Chem.* **1991**, *266*, 10246–10248.
 (4) Groves, J. T.; Haushalter, R. C.; Nakamura, M.; Nemo, T. E.; Evans, B. J. *J. Am. Chem. Soc.* **1981**, *103*, 2884–2886.
 (5) (a) Penner, J. E.; McMurry, T. J.; Renner, M.; Latos-Grazynski, L.; Smith, E. K.; Davis, I. M.; Hodgson, K. O. *J. Biol. Chem.* **1983**, *258*, 12761–12764. (b) Penner, J. E.; Smith, E. K.; McMurry, T. J.; Renner, M.; Balch, A. L.; Groves, J. T.; Hodgson, K. O. *J. Am. Chem. Soc.* **1986**, *108*, 7819–7825.
 (6) Boso, B.; Lang, G.; McMurry, T. J.; Groves, J. T. *J. Chem. Phys.* **1983**, *79*, 1122–1126.
 (7) (a) Balch, A. L.; Latos-Grazynski, L.; Renner, M. *J. Am. Chem. Soc.* **1985**, *107*, 2983–2985. (b) Balch, A. L.; Comman, C. R.; Latos-Grazynski, L.; Renner, M. *J. Am. Chem. Soc.* **1992**, *114*, 2230–2237.
 (8) (a) Hashimoto, S.; Tatsuno, Y.; Kitagawa, T. *J. Am. Chem. Soc.* **1987**, *109*, 8096–8097. (b) Hashimoto, S.; Mizutani, Y.; Tatsuno, Y.; Kitagawa, T. *J. Am. Chem. Soc.* **1991**, *113*, 6542–6549.
 (9) (a) Olmstead, M. M.; Cheng, R.-J.; Balch, A. L. *Inorg. Chem.* **1982**, *21*, 4143–4148. (b) Chevrier, B.; Weiss, R.; Lange, M.; Chottard, J.-C.; Mansuy, D. *J. Am. Chem. Soc.* **1981**, *103*, 2899–2901. (c) Latos-Grazynski, L.; Cheng, R.-J.; LaMar, G. N.; Balch, A. L. *J. Am. Chem. Soc.* **1981**, *103*, 4270–4272.
 (10) Bonnett, R. J.; Ridge, R.; Appelman, E. H. *J. Chem. Soc., Chem. Commun.* **1978**, 310–311.

- (11) (a) Balch, A. L.; Chan, Y.-W.; Olmstead, M. M. *J. Am. Chem. Soc.* **1985**, *107*, 6510–6514. (b) Balch, A. L.; Chan, Y.-W.; Olmstead, M. M.; Renner, M. W. *J. Am. Chem. Soc.* **1985**, *107*, 2393–2398.
 (12) (a) Tatsumi, K.; Hoffmann, R. *Inorg. Chem.* **1981**, *20*, 3771–3784. (b) Strich, A.; Veillard, A. *Nouv. J. Chim.* **1983**, *7*, 347–352. (c) Jorgensen, K. A. *J. Am. Chem. Soc.* **1987**, *109*, 698–705.
 (13) (a) Groves, J. T.; Watanabe, Y. *J. Am. Chem. Soc.* **1986**, *108*, 7836–7838. (b) Groves, J. T.; Watanabe, Y. *J. Am. Chem. Soc.* **1988**, *110*, 8443–8452.
 (14) Ortiz de Montellano, P. R.; Kunze, K. L. *Biochemistry* **1981**, *20*, 7266–7271. (b) Ortiz de Montellano, P. R. In *Cytochrome P-450*; Ortiz de Montellano, P. R., Ed.; Plenum Press: New York, 1986, pp 217–271.
 (15) Tsurumaki, H.; Watanabe, Y.; Morishima, I. *J. Am. Chem. Soc.* **1993**, *115*, 11784–11788.
 (16) Spiro, T. G. In *Resonance Raman Spectra of Biological Molecules*; John Wiley: New York, 1988; Vol. 3.

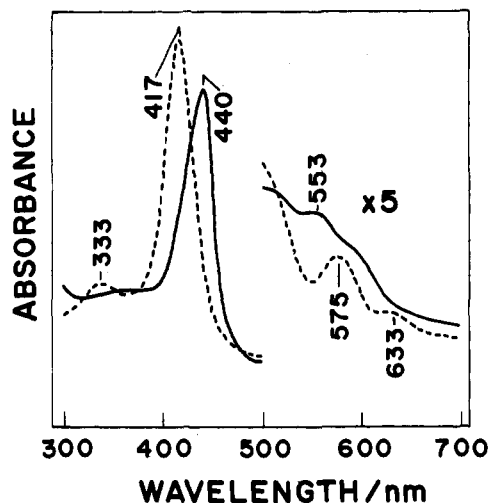


Figure 1. Visible absorption spectra of the parent compound, (TMP)- $\text{Fe}^{\text{III}}\text{OH}$ (broken line), and the product, (TMP) *N*-oxide (solid line).

derivatives [(TMP) $^{54}\text{Fe}^{\text{III}}\text{OH}$] were synthesized by a reported method.¹⁷ ^{18}O -labeled *m*-chloroperoxybenzoic acid (^{18}O -*m*-CPBA) was synthesized from *m*-chlorobenzoyl chloride and $\text{H}_2^{18}\text{O}_2$ in the presence of NaOH. The $\text{Fe}^{\text{III}}\text{-P}$ *N*-oxide was obtained through oxidation of (TMP) $\text{Fe}^{\text{III}}\text{OH}$ by *m*-CPBA in thoroughly degassed and dehydrated toluene,¹³ and its formation was confirmed by the visible absorption spectra.

Raman scattering was excited by a He/Cd laser (Kinmon Electronics, CD1801A) and recorded on a JEOL 400D Raman spectrometer, equipped with a cooled RCA-31034a photomultiplier. The Raman spectrometer was calibrated with indene (1600–700 cm^{-1}) and CCl_4 (700–200 cm^{-1}) as a standard. The temperature of the sample in the cylindrical cell was kept at 5 $^\circ\text{C}$ during the measurements. The visible absorption spectra were measured with an 1-mm-path-length cuvette and a Hitachi 220S spectrophotometer.

Results and Discussion

Figure 1 shows the visible absorption spectra of the initial compound [(TMP) $\text{Fe}^{\text{III}}\text{OH}$, broken line] and the *N*-oxide product (solid line). The spectrum shown by the solid line is in good agreement with that of the compound confirmed to be $\text{Fe}^{\text{III}}\text{-P}$ *N*-oxide with EPR and NMR spectroscopy.¹⁵

Figure 2 displays the RR spectra of the *N*-oxide isotope derivatives in the 680–220- cm^{-1} region. Traces a and c in Figure 2 show the RR spectra of the *N*-oxide obtained by ^{16}O -*m*-CPBA oxidation of (TMP) $^{\text{NA}}\text{Fe}^{\text{III}}\text{OH}$ and (TMP) $^{54}\text{Fe}^{\text{III}}\text{OH}$, respectively, and traces b and d are the ^{18}O -counterparts of traces a and c. The RR band at 507 cm^{-1} in trace a is downshifted to 498 cm^{-1} in trace b upon the $^{16}\text{O}/^{18}\text{O}$ substitution. Replacement of $^{\text{NA}}\text{Fe}$ with ^{54}Fe causes shifts of the RR bands from 507 cm^{-1} in trace a and 498 cm^{-1} in trace b to 508 cm^{-1} in trace c and 500 cm^{-1} in trace d, respectively. Since the frequency of this band is sensitive to the mass of both the Fe and O atoms, the 507- cm^{-1} band is assigned to $\nu_{\text{Fe-O}}$ of the *N*-oxide. This frequency is close to $\nu_{\text{Fe-O}}$ frequencies of $\text{Fe}^{\text{III}}\text{-P}$ hydroxy (490–495 cm^{-1})¹⁸ and methoxy (541 cm^{-1}) complexes.¹⁹ The observed isotopic shifts are smaller than that expected for a diatomic Fe–O molecule, indicating strong vibrational coupling with other modes.

Figure 3 displays the RR spectra of the *N*-oxide isotope derivatives in the 1200–700- cm^{-1} region. Traces a and c show RR spectra of the ^{16}O -*m*-CPBA-oxidized (^{14}N -TMP) $\text{Fe}^{\text{III}}\text{OH}$ and (^{15}N -TMP) $\text{Fe}^{\text{III}}\text{OH}$, while traces b and d are their ^{18}O -counterparts. In this frequency region three oxygen-isotope sensitive bands were observed at 1122, 743, and 708 cm^{-1} . When

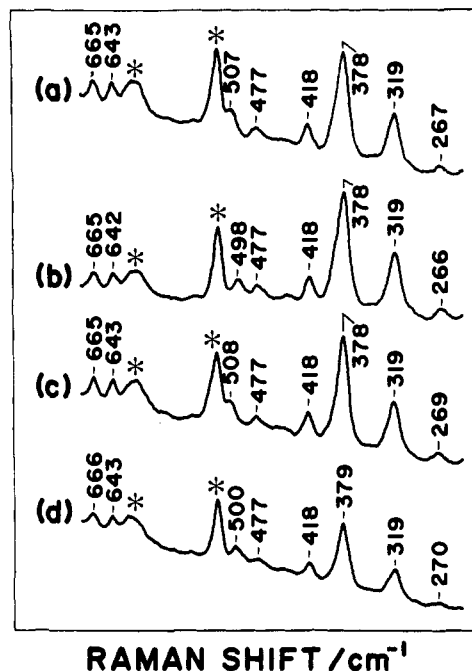


Figure 2. RR spectra of $\text{Fe}^{\text{III}}\text{-P}$ *N*-oxide isotope derivatives in the 680–220- cm^{-1} region: (a) $^{16}\text{O}/^{\text{NA}}\text{Fe}$ derivative; (b) $^{18}\text{O}/^{\text{NA}}\text{Fe}$ derivative; (c) $^{16}\text{O}/^{54}\text{Fe}$ derivative; (d) $^{18}\text{O}/^{54}\text{Fe}$ derivative. Asterisks denote the Raman bands of solvent.

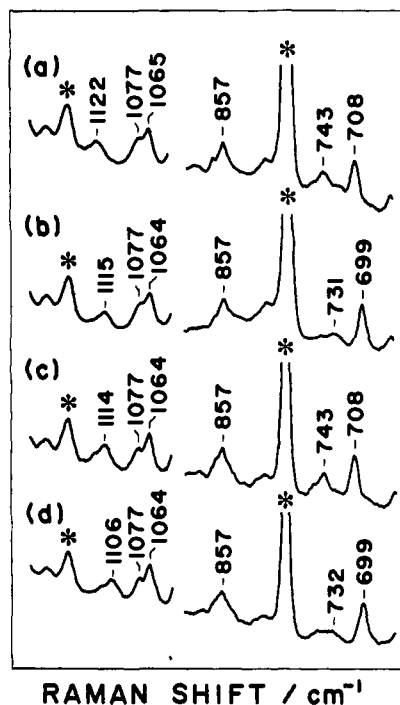


Figure 3. RR spectra of $\text{Fe}^{\text{III}}\text{-P}$ *N*-oxide isotope derivatives in the 1200–650- cm^{-1} region: (a) $^{16}\text{O}^{14}\text{N}$ derivative; (b) $^{18}\text{O}^{14}\text{N}$ derivative; (c) $^{16}\text{O}^{15}\text{N}$ derivative; (d) $^{18}\text{O}^{15}\text{N}$ derivative. Asterisks denote the Raman bands of solvent.

$^{16}\text{O}^{14}\text{N}$, $^{18}\text{O}^{14}\text{N}$, $^{16}\text{O}^{15}\text{N}$, and $^{18}\text{O}^{15}\text{N}$ derivatives are employed, the first band shifts to 1122, 1115, 1114, and 1106 cm^{-1} . Since the frequency shift in trace d from trace a is nearly the sum of those in traces b and c, this band is assigned to ν_{ON} . The second band was observed at 743, 731, 743, and 732 cm^{-1} and the third band at 708, 699, 708, and 699 cm^{-1} for $^{16}\text{O}^{14}\text{N}$, $^{18}\text{O}^{14}\text{N}$, $^{16}\text{O}^{15}\text{N}$, and $^{18}\text{O}^{15}\text{N}$ derivatives. Both bands behave similarly, being sensitive to ^{18}O - but not to ^{15}N -substitution, although the latter set are always weak and broad. Since the $\nu_{\text{Fe-O}}$ and ν_{ON} bands are singlets, it is unlikely to assume the presence of two forms.

(17) Cheng, R.-J.; Latos-Grazynski, L.; Balch, A. L. *Inorg. Chem.* **1982**, *21*, 2412–2417.

(18) (a) Asher, S. A.; Vickery, L. E.; Schuster, T. M.; Sauer, K. *Biochemistry* **1977**, *16*, 5849–5856. (b) Asher, S. A.; Schuster, T. M. *Biochemistry* **1979**, *18*, 5377–5387.

(19) Uno, T.; Hatano, K.; Nawa, T.; Nakamura, K.; Arata, Y. *Inorg. Chem.* **1991**, *30*, 4322–4326.

Presumably, the strong and sharp bands are assigned to the mode mainly containing δ_{FeON} , while the broad band is a coupled porphyrin mode (ν_{P}) whose unperturbed frequency is $\sim 731 \text{ cm}^{-1}$. Even if the ν_{P} mode is an out-of-plane mode with no Raman intensity under a planar structure, it may appear in a RR spectrum by borrowing intensity through vibrational mixing with δ_{FeON} , whose unperturbed frequency is 720 cm^{-1} for the $^{16}\text{O}^{14}\text{N}$ derivative. When δ_{FeON} is shifted to 699 cm^{-1} upon ^{18}O -substitution, the vibrational mixing becomes much less effective and its Raman intensity becomes weak. Since the pyrrole ring with the bridged nitrogen is tilted from the planar structure, the ν_{P} mode localized to the particular pyrrole might have some Raman intensity, as observed by spectra b and d. Broadness of this band might be due to inhomogeneity in the magnitude of tilting. Therefore, it is most likely that the intrinsic δ_{FeON} RR band has relatively strong Raman intensity and couples with a ν_{P} mode, presumably an out-of-plane mode which borrows RR intensity from δ_{FeON} .

Figure 4 compares the RR spectra of (TMP)Fe^{III}OH with those of the *N*-oxide. The bands of (TMP)Fe^{III}OH at 1361 and 1554 cm^{-1} (a), which are observed at 1355 and 1554 cm^{-1} for ($^{15}\text{N}_4$ -TMP)Fe^{III}OH (b), are assigned to ν_4 (C_αN stretching) and ν_2 ($\text{C}_\beta\text{C}_\beta$ stretching) modes, respectively.²⁰ Similarly, the RR bands of the *N*-oxide at 1364 and 1338 cm^{-1} (c), which are sensitive to pyrrole ^{15}N -substitution, are assigned to ν_4 and those at 1553 and 1537 cm^{-1} to ν_2 . The 1364- and 1553-cm^{-1} bands of spectrum c cannot be ascribed to unreacted (TMP)Fe^{III}OH, because its population, if present, should be very low in the absorption spectrum shown in Figure 1, and the excitation wavelength (441.6 nm) is much closer to the absorption maximum of the *N*-oxide (440 nm) than to that of (TMP)Fe^{III}OH (417 nm). The presence of two bands for each mode is consistent with the increase of asymmetry indicated by ^1H NMR^{13a} and EPR¹⁵ studies and would serve as a marker for *N*-oxide formation in P-450. Similar splittings of RR bands are also observed for metallotetraphenylchlorins with lower symmetry.²¹ The RR band at 1230 cm^{-1} in Figure 4a exhibits a downshift by 4 cm^{-1} upon *N*-oxidation (Figure 4c). This band arises from the C_m -phenyl

(20) Li, X.-Y.; Czernuszewicz, R. S.; Kincaid, J. R.; Su, Y. O.; Spiro, T. G. *J. Phys. Chem.* **1990**, *94*, 31–47.

(21) Andersson, L. A.; Locher, T. M.; Thompson, R. G.; Strauss, S. H. *Inorg. Chem.* **1990**, *29*, 2142–2147.

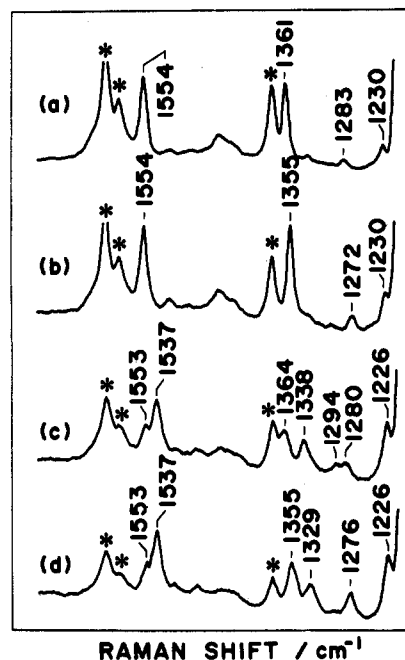


Figure 4. The RR spectra of (TMP)Fe^{III}OH and its *N*-oxide complex in the 1200–1700- cm^{-1} region: (a) unlabeled (TMP)Fe^{III}OH; (b) pyrrole- ^{15}N -labeled (TMP)Fe^{III}OH; (c) *N*-oxide species derived from unlabeled (TMP)Fe^{III}OH; (d) *N*-oxide species derived from pyrrole- ^{15}N -labeled (TMP)Fe^{III}OH. Asterisks denote the Raman bands of solvent.

stretching mode,²⁰ and its frequency is insensitive to a change in the spin and oxidation states of iron as well as to the formation of a π cation radical.^{8b,22} The 4-cm^{-1} downshift of this mode would indicate a considerable distortion of the macrocycle, as observed for the *N*-oxide of Ni-porphyrin.^{11a} In summary, we have assigned the Fe–O and O–N stretching and Fe–O–N bending resonance Raman bands. The results provide the first spectroscopic evidence for the Fe–O–N bridged structure of Fe(TMP) *N*-oxide.

(22) Mizutani, Y.; Hashimoto, S.; Tatsuno, Y.; Kitagawa, T. *J. Am. Chem. Soc.* **1990**, *112*, 6809–6814.